Impact of Moisture Distribution Within the Sensing Depth on L- and C-Band Emission in Sandy Soils

Pang-Wei Liu, *Student Member, IEEE*, Roger D. De Roo, *Member, IEEE*, Anthony W. England, *Fellow, IEEE*, and Jasmeet Judge, *Senior Member, IEEE*

***Abstract*—The performances of the soil moisture retrieval and assimilation algorithms using microwave observations rely on realistic estimates of brightness temperatures ($\mathbf{T_B}$) from microwave emission models. This study identifies circumstances when current models fail to reliably relate near-surface soil moisture to an observed $\mathbf{T_B}$ at L-band; offers a plausible explanation of the physical cause of these failures; and recommends improvements needed so that L-band observations can provide reliable estimates of soil moisture, more universally. Physically consistent soil parameters and moisture at the surface were estimated by using dual-polarized C-band observations during an intensive field experiment, for an irrigation event and subsequent drydown. These derived parameters were used in conjunction with the *in situ* moisture in deeper layers and different moisture profiles within the moisture sensing depth to obtain estimates of H-pol $\mathbf{T_B}$ at L-band, that provided best matches with the observed $\mathbf{T_B}$. The general assumptions of linear moisture distribution, with uniform or exponentially decaying weighting functions provided realistic $\mathbf{T_B}$ during the later stages of the drydown. However, the RMSDs of the $\mathbf{T_B}$s were upto 10.37 K during the wet period. In addition, the use of one value of moisture representing the entire moisture sensing depth during this highly dynamic stage of the drydown provides unrealistic estimates of emissivity, and hence, $\mathbf{T_B}$ at L-band. This study recommends use of a hydrological model to provide dynamic, realistic soil moisture profiles within the sensing depth and also an improved emissivity model that utilizes these detailed profiles for estimating $\mathbf{T_B}$.**

***Index Terms*—Emission models, moisture sensing depth, passive microwave remote sensing, rough surface emissivity, soil moisture profile.**

I. Introduction

WATER content in the root zone is a critical driver for hydrological processes and a governing factor in crop growth. Accurate estimation of the root zone soil moisture (RZSM) is essential for predicting moisture fluxes such as evapotranspiration, surface runoff, infiltration, and recharge, as well as crop growth and yield [1]. Because the relaxation frequency of liquid water lies in the microwave region, the dielectric constant exhibits large differences between wet and dry soils. Therefore, remotely sensed observations at microwave frequencies are sensitive to changes of the water content in the top layers of soil. Particularly, observations at the lower frequencies of L- (1.4 GHz) and C-band (6.7 GHz) are most applicable for soil studies because of negligible atmospheric attenuation, better penetration through vegetation, and greater sensitivity to moisture.

Satellite-based microwave systems allow frequent observations of global soil moisture. Currently, C-band observations from the Advanced Microwave Scanning Radiometer aboard the Earth Observation System (AMSR-E), available until October 2011, and from the Advanced SCATterometer (ASCAT) are being used to retrieve soil moisture at the spatial resolutions of 60 and 50 km, with repeat coverages of 2 and 5 days, respectively [2], [3]. The recently launched Soil Moisture and Ocean Salinity (SMOS) mission by the European Space Agency (ESA) [4] provides passive microwave observations at L-band with a spatial resolution of 40–50 km, with a repeat coverage of 2–3 days. In addition, the planned National Aeronautics and Space Administration (NASA) Soil Moisture Active Passive (SMAP) mission [5] will combine active and passive observations at L-band to provide global near-surface soil moisture at 9–36 km, with a repeat coverage of 2–3 days. Although both passive and active techniques measure the microwave radiation with similar sensitivities to soil moisture [6], the active technique is highly sensitive to the backscatter by soil roughness and vegetation [7]–[9], effectively masking much of the contribution from soil moisture. Consequently, the sensitivity to soil moisture will be primarily obtained from the passive technique at coarser spatial resolution of the radiometer, and radar will be used to estimate the sub-radiometer pixel variability of soil moisture.

The microwave emission from an unvegetated terrain, $\mathrm{T_B}$, is estimated as the sum of contributions from soil ($T_{Bsoil,p}$) and sky ($T_{Bsky,p}$), shown as:

$$T_B = T_{Bsoil,p} + T_{Bsky,p} \tag{1a}$$

$$T_{Bsoil,p} = e_p T_{eff} \tag{1b}$$

$$T_{Bsky,p} = T_{sky}(1 - e_p) \tag{1c}$$

where, p is either H- or V-polarization, T_{eff} is the effective temperature of bare soil, defined as an integral of radiative temperature over non-isothermal soil layers [10], e_p is effective emissivity of the soil within the moisture sensing depth (MSD), and

Manuscript received October 14, 2011; revised February 08, 2012, March 12, 2012, and May 16, 2012; accepted July 13, 2012. Date of publication October 18, 2012; date of current version May 13, 2013. This research was supported by the NASA-Terrestrial Hydrology Program (THP)-NNX09AK29G. Partial support for MicroWEX-5 was obtained from the NSF Earth Science Division (EAR-0337277) and the NASA New Investigator Program (NASA-NIP-00050655).

P.-W. Liu and J. Judge are with the Center for Remote Sensing, Agricultural and Biological Engineering Department, Institute of Food and Agricultural Sciences, University of Florida, Gainesville, FL 32603 USA (e-mail: bonwei@ufl.edu).

R. D. De Roo is with the Department of Atmospheric, Oceanic and Space Sciences, University of Michigan, Ann Arbor, MI 48109 USA.

A. W. England is with the Department of Atmospheric, Oceanic and Space Sciences, and the Department of Electrical Engineering and Computer Science, University of Michigan, Ann Arbor, MI 48109 USA.

Color versions of one or more of the figures in this paper are available online at http://ieeexplore.ieee.org.

Digital Object Identifier 10.1109/JSTARS.2012.2213239

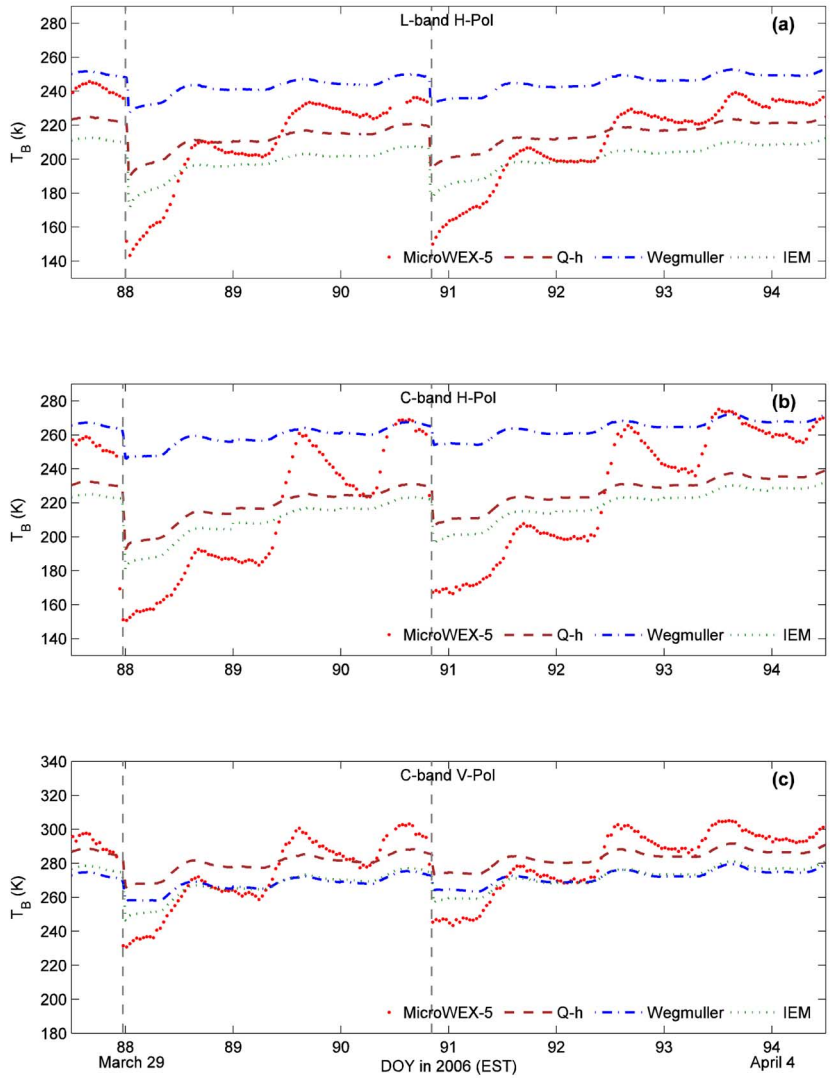

Fig. 1. Comparison of observed $\mathrm{T_B}$ from MicroWEX-5 (dots) with those estimated by Q-h (dashed line), Wegmüller (dash-dot line), and IEM models (dotted line) at (a) L-band H-pol, (b) C-band H-pol, and (c) C-band V-pol. For this simulation, the $s = 0.62$ cm, $cl = 8.72$ cm, and soil porosity $= 0.37$. Vertical dashed lines indicate irrigation events.

T_{sky} is downwelling sky brightness, usually set to 5 K [11]. The microwave emission models require knowledge of moisture and temperature distribution in the soil to estimate $\mathrm{T_B}$.

Current studies estimate e_p from rough soil using moisture in the top 0–2 or 0–5 cm, assuming a homogeneous soil over this depth. The moisture in the 0–2 or 0–5 cm, called near-surface moisture, is derived either from *in situ* measurements or from land surface models (LSMs) such as NOAH[1] [12], NASA Catchment model [13], or Land Surface Process (LSP) model [14]. *In situ* measurements are not available in most regions of the world and the sensors are not able to measure moisture with high vertical resolution from surface to about 2 cm of the soil. The impact of soil properties within the MSD on $\mathrm{T_B}$ is not well understood and several studies have used different approaches to obtain realistic estimates of $\mathrm{T_B}$. For example, Schneeberger *et al.* (2004) [15] added a transition layer on the top soil and obtained plausible dielectric constant by changing soil porosity in the transition layer. Their approach improved the consistency between the modeled and observed $\mathrm{T_B}$. However, the dielectric heterogeneities in the soil are not only impacted by porosity, but also impacted by moisture distribution and anisotropies in the top soil [16], and improving only the porosity at the surface may not be sufficient for accurate estimation of soil emission. Also, the moisture in the upper few centimeters is highly dynamic, particularly in sandy soils during and immediately following hydrologic events. Thus, the use of averaged moisture values can result in unrealistic $\mathrm{T_B}$ estimation. For example, Fig. 1(a)–(c) show that current state-of-the-art formulations are unable to provide realistic estimations of $\mathrm{T_B}$ at L- and C-band when compared with the observed $\mathrm{T_B}$ values for sandy soils. The $\mathrm{T_B}$ were estimated using the ϵ from [17], T_{eff} from [18], $\mathrm{T_B}$ from [19], [20] and [21], and using field observations of soil moisture at 0–2 cm, temperature at 0–2 and 64 cm, and surface roughness in sandy soils of North Central Florida [22]. During the simulation period from noon March 28, Day of Year (DoY) 87.5,

[1]NOAH represents National Centers for Environmental Prediction (NCEP), Oregon State University (OSU), Air Force, and Hydrologic Research Laboratory.

to noon April 4 (DoY 94.5), the field was irrigated at the midnight of March 29 (DoY 87.97) and in the late evening of April 1 (DoY 90.82). The models overestimate H-pol T_B at L-band by as much as 82 K, and C-band T_B at H- and V-pol by 96 K and 34 K, respectively, at the time of the event. During the entire simulation period, the Root Mean Square Differences (RMSDs) between the modeled and the observed T_B at L-band were 17.16 K, 37.80 K, and 20.47 K, using rough surface formulations [19], [20] and [21], respectively.

Such unrealistic T_B estimates from soil have potentially significant impacts on the performance of data assimilation and soil moisture retrieval algorithms, for both bare and vegetated surfaces. Because most current models are calibrated to expected norms, these algorithms are most likely to fail during extremes of wet and dry hydrological conditions. Wet extremes include the few hours up to a day of drydown immediately following a hydrologic event, and dry extremes occur when normally moist near-surface soils have become desiccated of their free-water during near-drought conditions. The implications of the findings of this study for reliably estimating soil moisture from microwave brightness are important because it is often during these extremes that reliable estimates are most relevant.

The goals of this study are to understand the sources of differences between the modeled and the observed brightness temperature during hydrologic events and during early stages of the drydown; and to further explore the near-surface moisture profiles and estimation of rough surface emissivities at L-band in sandy soils. The objectives are to (1) obtain a plausible soil moisture profile consistent with C- and L-band observations during two drydown periods for sandy soils, (2) provide insights into physical causes of unrealistic T_B estimates, and (3) recommend improvements that are necessary in the microwave brightness models to achieve reliable soil moisture retrieval and assimilation algorithms. In Section II, we describe the field observations used in this study. The emission models, and the methodology for estimating soil properties and T_B at C- and L-band are described in Section III. In Sections IV and V, results are discussed and summarized, respectively.

II. Experimental Observations

Microwave Water and Energy Balance Experiments (MicroWEXs) are a series of season-long experiments conducted at Plant Science Research and Education Unit (PSREU), Institute of Food and Agricultural Sciences (IFAS), in north central Florida, to monitor the microwave signatures of soil and vegetation during different stages of growth [22]–[25]. This study used the bare soil observations during the fifth MicroWEX (MicroWEX-5), conducted during a growing season of sweet corn from March 9 (DoY 68) to May 26 (DoY 150), 2006 [22]. The soil physical properties observed at the site are given in Table I. During the experiment, T_B were observed at 1.4 and 6.7 GHz ($\lambda = 21.0$ and 4.48 cm), with an incidence angle of 50°, using two tower-mounted radiometers: the UF L-band Microwave Radiometer (UFLMR) and the UF C-band Microwave Radiometer (UFCMR). Table II lists specifications of the two radiometer systems. The 15-minute microwave observations were augmented with concurrent observations of soil temperature and moisture values at different depths in the soil profile, as shown in Table I. Four rain gauges were used to record the amount of water during the irrigation/precipitation events. Fig. 2 shows the field site and sensor layout during MicroWEX-5. Soil roughness measurements, including root mean square height (s) and correlation length (cl), as listed in Table III, were conducted using a 2-m-long mesh board and a ground-based Light Detection And Ranging (LiDAR) system [26]. In this study, observations from noon March 28 (DoY 87.5) to noon April 4 (DoY 94.5) were used, during which the Leaf Area Index (LAI) was <0.3. Details of other observations during the MicroWEX-5 experiment are provided in [22].

TABLE I
Measurements of Soil Properties During MicroWEX-5

MicroWEX-5 Soil Observations	
Physical Properties	• Texture: – Sand = 89.4% by vol – Clay=7.17% by vol – Silt=3.5% by vol • Bulk density: 1.67 g/cm^3
Moisture & Temperature Profiles	• Depths: 2, 4, 8, 16, 32, 64, and 120cm

TABLE II
Specifications of the UF L-Band Microwave Radiometer (UFLMR) and the UF C-Band Microwave Radiometer (UFCMR)

Parameter	Qualifier	UFLMR	UFCMR
Frequency(GHz)	Center	1.4	6.7
Bandwidth(MHz)	3dB	20	20
Beamwidth(deg)	3dB	22.5	23
Polarization	Sequential	H	V/H
Noise Figure(dB)	From T_{rec}	3.99	3.99
RF Gain(dB)		79	85

TABLE III
Soil Surface Roughness Measurements of Root Mean Square Height (s) and Correlation Length (cl) Using Mesh Board and Ground-Based LiDAR During MicroWEX-5

DoY	Mesh Board		LiDAR	
(2006)	s (cm)	cl (cm)	s (cm)	cl (cm)
67	0.8	15.5	0.7	11.3
69	0.7	8.1	0.7	9.1
69	0.4	5.3	0.4	3.0

III. Methodology

A. Microwave Brightness (MB) Models

The microwave brightness model estimates contributions from soil and sky ((1a)–(1c)). The sky contribution is very small and set to 5 K. The soil is assumed as a non-isothermal, semi-infinite layered dielectric medium, with a rough surface at the upper boundary. The incoherent solution for the microwave brightness temperature of such a soil accounts for reflections at layer-interfaces, and the propagation of the radiance through each layer, as shown in Fig. 3. The brightness temperature above the layer j, T_{Bj}, is given as:

$$T_{Bj} = \begin{Bmatrix} T_{Bj}^{+} \\ T_{Bj}^{-} \end{Bmatrix} = B_{j,j+1} T_{Bj+1} + S_{j+1} \tag{2a}$$

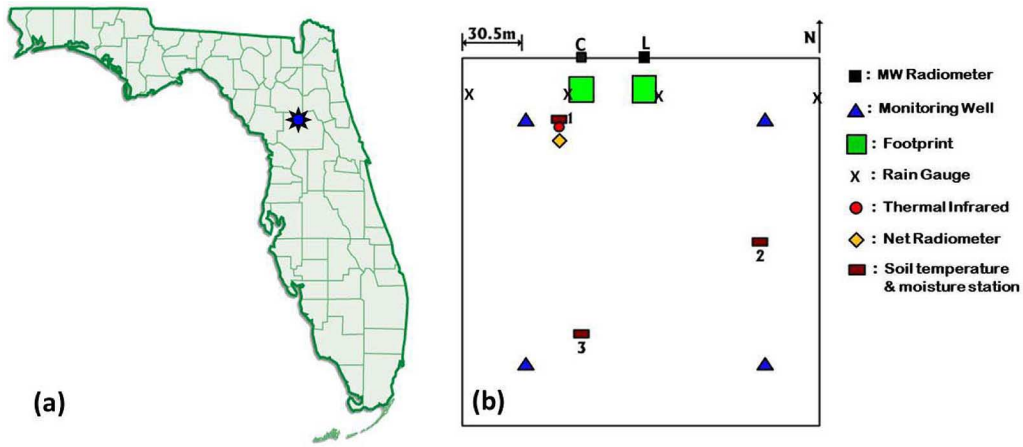

Fig. 2. (a) Location of the experimental field, as marked with a star, at the Plant Science Research and Education Unit (PSREU) in North Central Florida, and (b) sensor layout during MicroWEX-5.

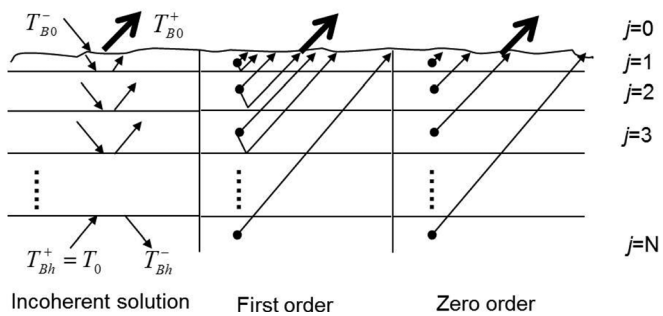

Fig. 3. The illustrations of the incoherent solution of the radiative transfer equation, first-order, and zero-order approximations for estimating emission from a layered soil with infinite lower boundary.

where, T_{Bj}^+ and T_{Bj}^- are upwelling and downwelling brightness temperatures immediately above the j^{th} interface, respectively. $B_{j,J+1}$, the backward propagation matrix defined in (2b), represents reflection and extinction from the $j+1$ layer reaching the j^{th} layer. The second term, S_{j+1}, is the emission contribution from the $j+1^{th}$ layer, defined in (2c).

$$B_{j,j+1} = \frac{1}{1-R_j}\begin{Bmatrix} \frac{(1-2R_j)}{L_{j+1}} & R_j L_{j+1} \\ \frac{-R_j}{L_{j+1}} & L_{j+1} \end{Bmatrix} \tag{2b}$$

$$S_{j+1} = T_{j+1}\frac{1-\frac{1}{L_{j+1}}}{1-R_j}\begin{Bmatrix} 1-R_j(2+L_{j+1}) \\ -(R_j+L_{j+1}) \end{Bmatrix} \tag{2c}$$

where, R_j is the amplitude of reflection at the interface between the j^{th} and the $j+1^{th}$ layers, T_{j+1} is the physical temperature of the $j+1^{th}$ layer, and L_{j+1} is the loss factor of the $j+1^{th}$ layer, expressed as $L_{j+1} = exp(\kappa_{j+1}\triangle z_{j+1} sec\theta_{j+1})$, where κ_{j+1} is the absorption coefficient of the $j+1^{th}$ layer, $\triangle z_{j+1}$ is the thickness of the $j+1^{th}$ layer, and θ_{j+1} is the refractive angle between the interfaces of the j^{th} and $j+1^{th}$. The upwelling and downwelling brightness temperatures of the bottom, semi-infinite layer, N, as shown in Fig. 3, is a special case, where the upwelling brightness temperature, T_{Bh}^+, is equal to the physical temperature of the N^{th} layer, T_N, and the downwelling brightness temperatures, T_{Bh}^-, is unknown. So that, $T_{BN} = B_N T_{Bh}$, where:

$$B_{N,h} = \frac{1}{1-R_N}\begin{Bmatrix} (1-2R_N) & R_N \\ -R_N & 1 \end{Bmatrix} \tag{2d}$$

$$T_{Bh} = \begin{Bmatrix} T_N \\ T_{Bh}^- \end{Bmatrix} \tag{2e}$$

Setting the downwelling sky brightness temperature, T_{B0}^-, to zero, T_{B0}^+ becomes $T_{Bsoil,p}$ from a specular soil surface. The rough surface brightness temperature can be expressed:

$$T_{Bsoil,p} = e_p \frac{T_{B0}^+}{1-R_0} \tag{3}$$

First-order or zero-order approximations to propagation (2a) are often used in which either single reflections at interfaces are considered or reflections are ignored, respectively. The first-order approximation is given as [27]:

$$T_{Bsoil,p} = e_p \sum_{j=1}^{N} T_j \left(1-\frac{1}{L_j}\right)\left(1+\frac{R_j}{L_j}\right)\prod_{i=2}^{j}\left(\frac{(1-R_{i-1})}{L_{i-1}}\right) \tag{4}$$

The zero-order approximation that does not account for any reflections between the soil layers is given as [10]:

$$T_{Bsoil,p} = e_p \sum_{j=1}^{N} T_j \left(1-\frac{1}{L_j}\right)\prod_{i=2}^{j}\frac{1}{L_{i-1}} \tag{5}$$

All of these models use complete soil moisture and temperature profiles for the $T_{Bsoil,p}$ estimation, when such measurements are available, and allow for user-defined thickness of soil layers. In this study, the backward propagation solution and its two approximations are compared and discussed to understand the applicability of the approximations in estimating realistic L-band T_B of the sandy soils.

B. Rough Surface Emissivity Model

Although the semi-empirical approaches for rough surface emissivities [18], [19], [28]–[32] are widely used, such as for

the SMOS mission, the model parameters in these approaches are highly dependent upon the observations used during the regression process. In order to avoid such uncertainties, a more physically-based, Integral Equation Model (IEM) [21], is used in this study, to estimate the rough surface emissivity. The emissivity is defined as:

$$e_p = 1 - \left(r_p^{non}(\theta_0) + r_p^{coh}(\theta_0)\right) \tag{6}$$

where, $r_p^{non}(\theta_0)$ and $r_p^{coh}(\theta_0)$ are noncoherent and coherent reflectivities at the incidence angle, θ_0, respectively, and they can be written as:

$$r_p^{non}(\theta_0) = \frac{1}{4\pi cos\theta_0} \int_0^{2\pi} \int_0^{\frac{\pi}{2}} \left[\sigma^0_{soil,pp}(\theta_0, \phi_0; \theta_s, \phi_s) + \sigma^0_{soil,qp}(\theta_0, \phi_0; \theta_s, \phi_s)\right] sin\theta_s d\theta_s d\phi_s \tag{7a}$$

$$r_p^{coh}(\theta_0) = r_{p0}(\theta_0) exp\left[-(2kscos\theta_0)^2\right] \tag{7b}$$

where, $\sigma^0_{soil,qp}$ is the bistatic scattering coefficient, (θ_0, ϕ_0) and (θ_s, ϕ_s) are elevation and azimuth angles for the incidence and the scattering radiation, respectively, r_{p0} is the Fresnel reflectivity, and s is the root mean square height. Fung *et al.* (1994) [21] derived an approximate solution for the scattering coefficient and proposed an emission model based upon the IEM. The model is applicable to a wide range of roughness and frequencies [33], and for a variety of natural terrains.

Note that all the current approaches estimate e_p using a single soil moisture value within the moisture sensing depth (MSD), also referred to as the surface layer, where the soil is assumed homogeneous. The MSD is defined as the depth at which the emission is 1/e described to $\delta_p = 1/\kappa$. Such a definition does not account for the reflections between soil layers, so the actual MSD may be different than the $\delta = 1/\kappa$.

C. Dielectric Constant Model

Dielectric constant, ϵ, of the wet soil is a function of soil components such as soil solids, water, and air. A semi-empirical model, developed by Dobson *et al.* (1985) [34], is widely used to estimate the ϵ for frequencies from 1.4 to 18 GHz. Recent studies have found that the Dobson *et al.* (1985) model significantly overestimates ϵ in sandy soils [17], [18]. Furthermore, the model proposed in [20] based their empirical radiative transfer model upon [34], and are not applicable for sandy soils. Mironov *et al.* (2009) [17] proposed a refractive mixing model for moist soils, shown as:

$$n_{soil} = \begin{cases} n_d + (n_b - 1)m_v & m_v \le m_{vt} \\ n_d + (n_b - 1)m_{vt} & \\ +(n_f - 1)(m_v - m_{vt}) & m_v > m_{vt} \end{cases} \tag{8a}$$

$$k_{soil} = \begin{cases} k_d + k_b m_v & m_v \le m_{vt} \\ k_d + k_b m_{vt} & \\ +k_f(m_v - m_{vt}) & m_v > m_{vt} \end{cases} \tag{8b}$$

where, n is the refractive index (RI), k is the normalized attenuation coefficient (NAC), the subscripts $soil$, d, b, and f refer to the soil, dry soil, bound water, and free water, m_v is the soil water content, and m_{vt} is the fraction of the maximum bound water. The mineralogically based equations for the RI and NAC of each element mentioned above are formed and listed in [17]. The dry soil component in (8a) and (8b) is a combination term of solid soil and air, and depends only upon the soil type. However, even for the same soil type, the soil porosity may vary with the soil column, changing the volume fraction of the soil solids.

In this study, we re-wrote the (8a) and (8b) in terms of soil porosity as:

$$n_{soil} = \begin{cases} n_{ss}\frac{\rho_b}{\rho_s} + n_b m_v + v_a & m_v \le m_{vt} \\ n_{ss}\frac{\rho_b}{\rho_s} + n_b m_{vt} & \\ +(n_f - 1)(m_v - m_{vt}) + v_a & m_v > m_{vt} \end{cases} \tag{9a}$$

$$k_{soil} = \begin{cases} k_{ss}\frac{\rho_b}{\rho_s} + k_b m_v & m_v \le m_{vt} \\ k_{ss}\frac{\rho_b}{\rho_s} + k_b m_{vt} & \\ +k_f(m_v - m_{vt}) & m_v > m_{vt} \end{cases} \tag{9b}$$

where, n_{ss} and k_{ss} are the real (RI) and imaginary (NAC) parts of $\sqrt{\epsilon_{ss}}$ from [34]. n_b, k_b, and m_{vt} are obtained from empirical soil models in [17], and n_f and k_f can be calculated from the Debye relaxation equations [11].

D. The Simulations

Two drydown periods, with varying water applications, were chosen for this study. The first drydown period, from noon March 31 (DoY 90.5) to noon April 4 (DOY 94.5), with 5 mm of water input on in the late evening of March 31 (DoY 90.8), consisted of 480 observations of H- and V-pol $\mathrm{T_B}$ at C-band and 375 observations of H-pol $\mathrm{T_B}$ at L-band; and the second drydown period from noon March 28 (DoY 87.5) to noon March 31 (DoY 90.5), with 7.5 mm water input at the midnight of March 30 (DoY 88.0), consisted of 281 observations of $\mathrm{T_B}$ at C-band and 282 observations of $\mathrm{T_B}$ at L-band.

Typically, the top-most layer of sandy soils consists of loose sand particles, with high porosity compared to the lower soil medium. In addition, due to its shorter wavelength, the C-band radiometric observations are highly sensitive to the properties at the surface, such as the roughness, porosity, water content in the shallower soil. The soil roughness, porosity, and moisture within the MSD were derived from the dual pol $\mathrm{T_B}$ observations at the C-band, as described in the section below. As shown in Fig. 4, the thickness of the soil layers in the top 2.5 cm was set to 1 mm to capture the strong dynamics of the moisture. The soil below 2.5 cm was divided into 1 cm-thick layers up to 64.5 cm and a semi-infinite layer below 64.5 cm. The soil moisture observations at the depths of 2, 4, 8, 16, 32, 64, and 120 cm from MicroWEX-5 represented the values for the modeled layers at 1.9–2.1, 3.5–4.5, 7.5–8.5, 15.5–16.5, 31.5–32.5, 63.5–64.5, and below 64.5 cm, respectively, as shown in Fig. 4. Soil moisture values in the other layers were obtained by linearly interpolating the values between the layers. The soil temperature observed at 2 cm during MicroWEX-5 was used as the temperature for the modeled layers from 0 to 2.5 cm. The temperatures for deeper layers, >2.5 cm were assigned in a similar manner to the soil moisture values.

E. Extracting Soil Parameters Using C-Band Signatures

1) Estimation of Surface Roughness and Soil Porosity Within MSD at C-Band: The initial MSD of C-band was set to 2 mm to estimate soil properties and the moisture consistent with

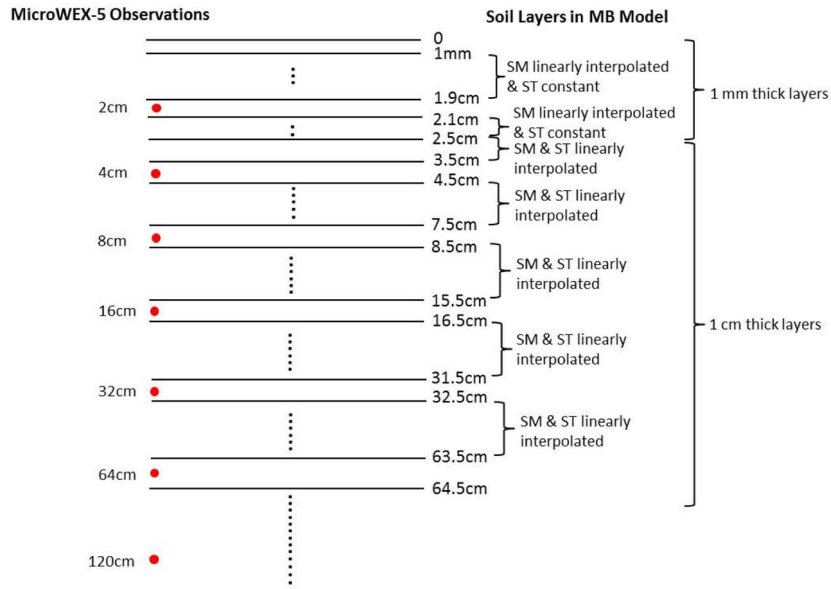

Fig. 4. Distribution of moisture and temperature in the soil layers of the MB model and corresponding observations at the depths of 2, 4, 8, 16, 32, 64, and 120 cm during MicroWEX-5.

dual-pol observations of C-band during the drydown period. The sensitivity of microwave emission to surface roughness increases as the soil gets wetter [33]. Therefore, the roughness properties, s and cl, were estimated during the driest period of the first drydown, around noon on April 3 (DoY 93.5), and were further refined during the wettest period, around midnight on April 1 (DoY 91), to ensure that the estimated values provided realistic $\mathrm{T_B}$ estimates during the entire drydown period. During the driest period, the soil moisture within the MSD was set to 0.01 $\mathrm{m^3/m^3}$ because the surface of the sandy soil is extremely dry due to insolation. The means of s and cl observations using mesh board and LiDAR during MicroWEX-5 were 0.62 and 8.72 cm with standard deviations of 0.17 and 4.42 cm, respectively. The initial values of surface roughness, s and cl, and porosity were set to 0.62, 8.72 cm, and 0.37, respectively, as observed during MicroWEX-5. Because the microwave emission is more sensitive to rms height, s, than the correlation length, cl, only s and porosity were adjusted to provide the lowest root mean square difference (RMSD) between the observed and the modeled $\mathrm{T_B}$. During the wet period, the value of s was further adjusted along with soil moisture value. Porosity was fixed at its value during the dry period.

2) Estimation of Soil Moisture Within the MSD at C-Band During the Drydown Period: These best estimates of s, cl, and porosity, found during the driest period, were implemented during the wettest period of the drydown, immediately after the irrigation event. The soil moisture and s values that provided the $\mathrm{T_B}$ estimates closest to the observed $\mathrm{T_B}$ were chosen during this wettest period, constrained by the porosity values estimated for the dry soil. The soil moisture within the moisture sensing depth was estimated during the drydown by dividing the drydown into several small intervals, with breaking points based upon temporal changes in the observed $\mathrm{T_B}$ at C-band. The best estimate of the soil moisture within MSD of C-band was determined by comparing the modeled and the observed $\mathrm{T_B}$ values at both V- and H-pol. The soil moisture values estimated at the breaking points were linearly interpolated to obtain continuous values during the entire drydown period.

F. Estimating T_B at L-Band

The current MB models use single soil moisture value, m_{v_f}, within the MSD, for estimating e_p to estimate $\mathrm{T_B}$, given as:

$$m_{v\_f} = \int_0^\infty m_v(z)w(z)dz \tag{10}$$

where, f represents the frequency, f, $m_v(z)$ is the soil moisture as a function of soil depth z, and $w(z)$ is the weighting function, with $\int_0^\infty w(z)dz = 1$.

In this study, we explore uniform and exponentially decaying weighting functions, given as:

$$w_u(z) = \begin{cases} \frac{1}{z_f} & 0 \le z \le z_f \\ 0 & z_f < z \end{cases} \tag{11}$$

and

$$w_e(z) = \frac{1}{z_f} exp\left(\frac{-z}{z_f}\right) \quad 0 \le z \le \infty \tag{12}$$

where, the subscripts u and e represent uniform and exponential, and z_f is the MSD at the frequency of f.

Using (9b), the ratio of the MSD at C- and L-band is a constant equal to 12.6 for different values of soil moisture, as shown in Table IV. Given the 2 mm MSD assumed at C-band, the MSD at L-band is 2.5 cm. The weighting functions can be applied to the discrete soil medium and the (10) becomes:

$$m_{v\_L} = \frac{\sum_{j=1}^{N} m_{vj}}{N} \tag{13}$$

TABLE IV
THE SOIL PENETRATION DEPTH (δ_p) OF C- AND L-BAND AND THE SENSING DEPTH RATIO

Soil moisture	δ_p of C-band (cm)	δ_p of L-band (cm)	Sensing depth ratio
0.01	21.22	267.35	12.60
0.05	4.24	53.47	12.61
0.1	2.12	26.74	12.61
0.2	1.06	13.37	12.61
0.3	0.71	8.91	12.55

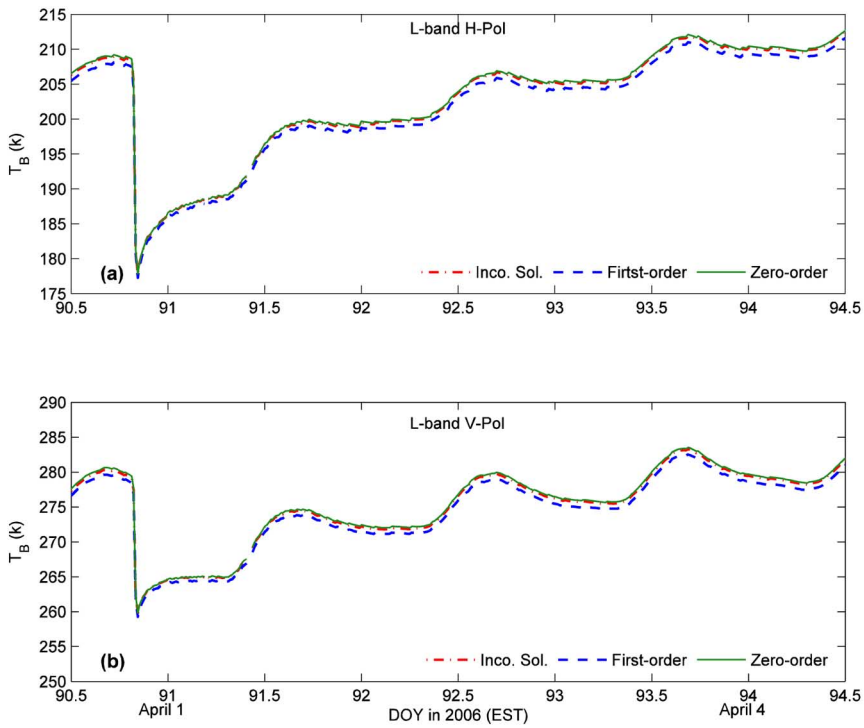

Fig. 5. Estimated $\mathrm{T_B}$ at L-band for the incoherent solution (dash-dot line), first-order (dashed line), and zero-order (solid line) approximations, for (a) H- and (b) V-pol using the soil moisture and temperature profiles observed during MicroWEX-5.

using uniform weighting function, and

$$m_{v\_L} = \frac{\sum_{j=1}^{N} m_{vj} W_{ej}}{\sum_{j=1}^{N} w_{ej}} \tag{14}$$

using exponentially decaying function. Where, L represents frequency at L-band, j is the j^{th} layer of soil, N is the soil layer at the MSD of L-band, W_{ej} is the soil moisture in the j^{th} layer of soil, and w_{ej} is the weight given to j^{th} layer of soil. The $m_v L$ is used to estimate e_p from IEM model and the $\mathrm{T_B}$ at L-band.

IV. RESULTS AND DISCUSSION

A. Comparison of the MB Models

Figs. 5(a) and (b) show the estimated L-band $\mathrm{T_B}$ at H- and V-pol, respectively, using the incoherent solution from (2) and (3), the first-order from (4), and the zero-order approximations from (5). These estimates were obtained with the 0–2 cm soil moisture and temperature observed during MicroWEX-5, and interpolated values for the layers below, as explained in Section III-D. The $\mathrm{T_B}$ estimates from the three approaches are very similar, with the maximum difference of <1.2 K among them. This indicates that the reflections between the soil layers may not be significant in the soil column of the sandy soils at the MicroWEX-5 site. In this study, we use the first-order approximation to account for the single reflection that may become significant at the interfaces of the sandy soil, where the moisture in the top surface is highly dynamic.

B. Estimating Surface Parameters From C-Band Signatures

1) Estimation of Surface Roughness and the Soil Porosity in the Top 0–2 mm: In the IEM model, the $\mathrm{T_B}$ at H-pol increases with roughness, while that at V-pol decreases [33]. In addition, the $\mathrm{T_B}$ increases with porosity and decreases with increasing soil moisture. Increasing the surface porosity results in an increased dynamic range of soil moisture at the surface. These relationships in the IEM model were used to determine the s and cl that were within observed ranges during the MicroWEX-5. The s and cl of 0.73 and 8.72 cm were found to provide the best $\mathrm{T_B}$ estimations during the driest period, from DoY 92.5–94.5, but the $\mathrm{T_B}$ were still underestimated by up to 13 K at H-pol and by up to 5 K at V-pol, when compared with the observed values. However, when soil porosity was increased to 0.55 in the top 2 mm, consistent with typical loose top layer in sandy soils, the best estimate of $\mathrm{T_B}$ was obtained during the driest period.

2) Estimation of Moisture in the Top 0–2 mm of Soil During the Drydown: The parameters, $s = 0.73$ cm, $cl = 8.72$ cm, and

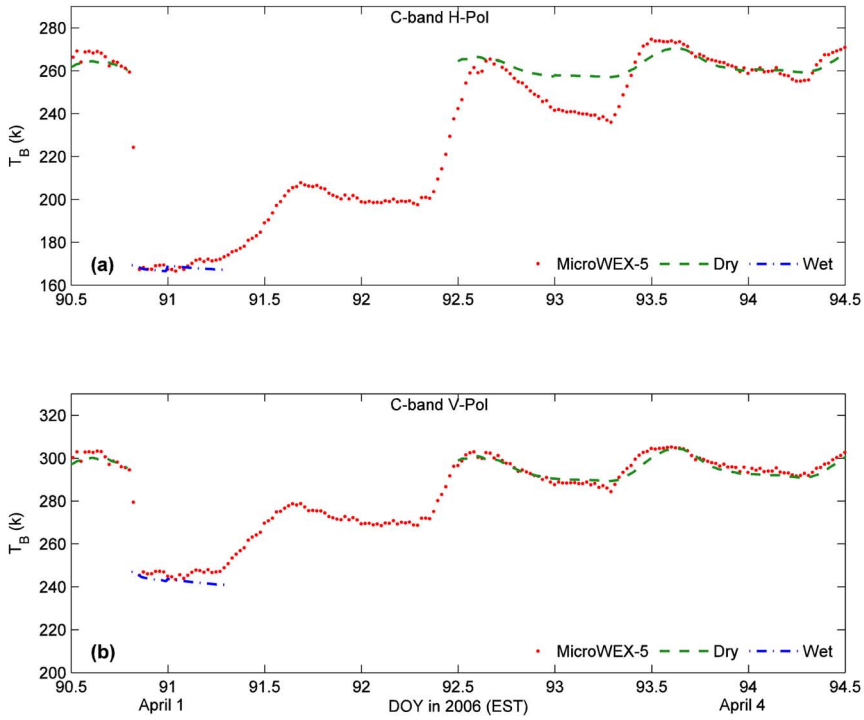

Fig. 6. Comparison of observed $\mathrm{T_B}$ from MicroWEX-5 (dots), with modeled $\mathrm{T_B}$ during the driest (dashed line), and the wettest periods (dash-dot line) at C-band for (a) H- and (b) V-pol using the s, cl, and porosity estimated during the driest period and moisture estimated during the wettest period.

$\mathrm{soil\ porosity} = 0.55$ found during the dry period, were applied during the wet period, from DoY 90.82 to 91.3, to find the water content in the top 0–2 mm of soil. The soil moisture value of 0.3 $\mathrm{m^3/m^3}$ in the top 2 mm during the wet period provided the best $\mathrm{T_B}$ estimations, even though they were overestimated by up to 12 K at H-pol, and those at the V-pol were underestimated by up to 10 K. A further decrease in s to 0.41 cm resulted in a better $\mathrm{T_B}$ estimate during both the wet and the dry periods, as shown in Fig. 6. The estimated value of s is close to one standard deviation of the observed s values during MicroWEX-5.

Ten breaking points were selected during the drydown period to obtain the water content in the top 0–2 mm of soil that resulted in the best H- and V-pol $\mathrm{T_B}$ estimates at C-band at those points. Fig. 7 shows the moisture values found at the breaking points, and the best estimated H- and V-pol $\mathrm{T_B}$ at C-band with the new soil moisture values in the top 0–2 mm. The RMSD of the H- and V-pol $\mathrm{T_B}$ were 2.67 K and 2.43 K, and standard deviations were 2.63 K and 1.70 K, respectively, when compared with the $\mathrm{T_B}$ observed during the MicroWEX-5. In Fig. 8, the soil moisture in the top 0–2 mm is compared to that observed at 2 and 4 cm during MicroWEX-5. As expected, the dynamic range near the surface is much larger than the range at the deeper layers. In addition, the $\mathrm{T_B}$ estimates at L-band using the IEM model, shown in the Fig. 1, suggest that a wetter soil surface during the wet periods and a drier soil surface during the dry periods were observed than predicted by models.

C. Impacts of Soil Moisture Distribution on Microwave Signatures at L-Band

The soil properties of s, cl, porosity, and soil moisture in the surface layer, obtained using C-band observations in the Section IV-B were used to estimate H-pol $\mathrm{T_B}$ at L-band using different moisture profiles within the MSD at L-band, as shown in Fig. 9. The soil moisture for the layers below the MSD at C-band was the same as given in Section III-D. The estimates of $\mathrm{T_B}$ were compared to those observed during MicroWEX-5 to gain insights into the impacts of the distribution of soil moisture on the microwave signatures and understand the assumptions necessary to match the observations. In Fig. 11, the observed $\mathrm{T_B}$ at L-band during MicroWEX-5 is compared with the estimates of $\mathrm{T_B}$ using different moisture profiles. The *first moisture profile* consisted of soil moisture 0–2 cm from observed value during MicroWEX-5, as shown in Fig. 10(a), with the newly estimated soil physical properties to understand the effect of only physical properties. The estimated $\mathrm{T_B}$, shown as the green dashed line in Fig. 11(a), show that the difference of overall estimates of $\mathrm{T_B}$ is within 2 K to the result shown in the Fig. 1 using original soil physical properties (see Table V). The result implies that the H-pol $\mathrm{T_B}$ estimates at L-band remain largely unaffected when only soil physical properties are changed, and the soil moisture observed at 2 cm is insufficient to represent the highly dynamic of soil moisture.

The *second moisture profile* was obtained by linearly interpolating the soil moisture values in 0–2 mm estimated from C-band, and those observed at 2 and 4 cm during MicroWEX-5, as shown in Fig. 10(b). Using this profile, the average soil moisture within the 0–2.5 cm, i.e. 12.6 times the MSD at C-band, was used to estimate rough surface emissivity. Thus this method weighs each layer within the MSD equally, using a uniform weighting function. The overall $\mathrm{T_B}$, shown as blue dashed line in Fig. 11(a), match the observations well with an RMSD of 4.53 K and SD of 4.52 K. This indicates that the overall dynamics $\mathrm{T_B}$ during the drydown could be captured using the

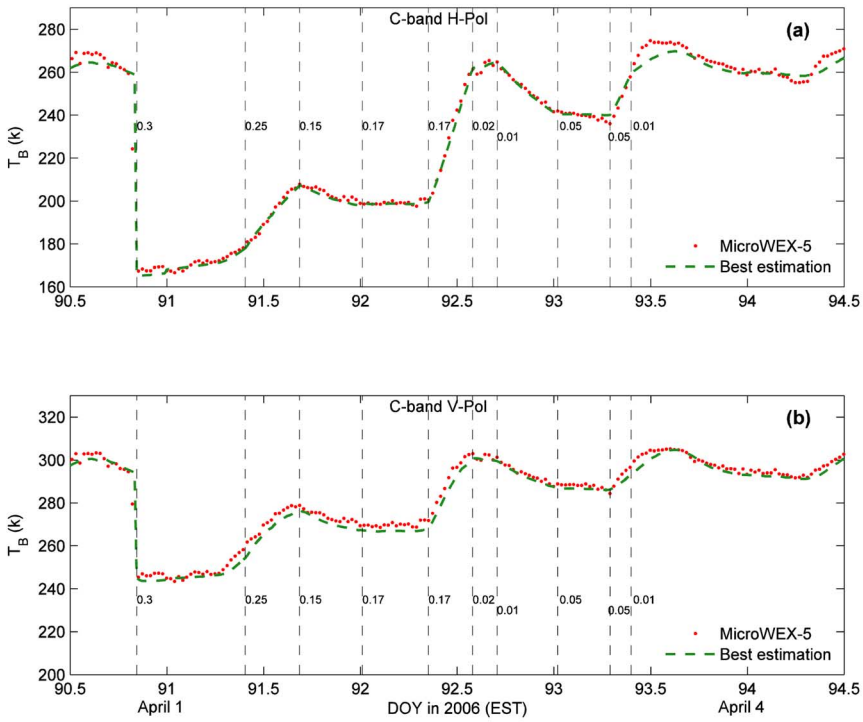

Fig. 7. The comparison of observed $\mathrm{T_B}$ from MicroWEX-5 (dot), and estimated $\mathrm{T_B}$ (dashed line) at C-band for (a) H- and (b) V-pol, and the ten breaking points (vertical dashed lines), with their associated soil moisture values (in $\mathrm{m^3/m^3}$) in the top 2 mm.

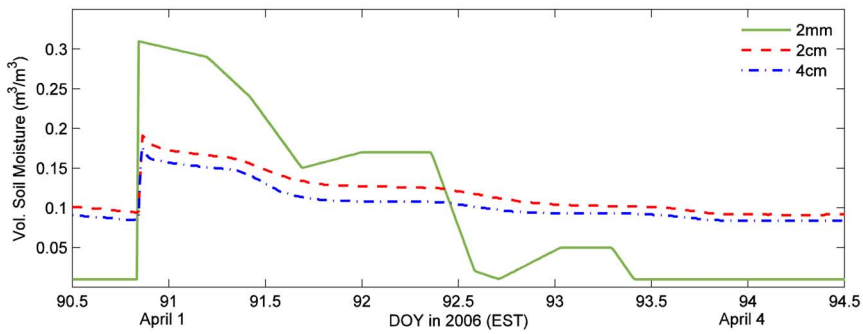

Fig. 8. The comparison of soil moisture estimated in the top 0–2 mm (solid line) and observations at 2 cm (dashed line) and 4 cm (dash-dot line) during MicroWEX-5.

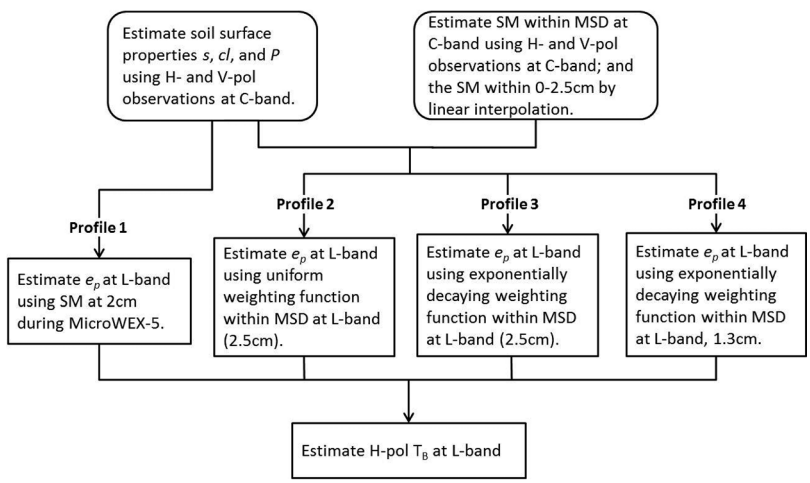

Fig. 9. The flow chart of steps to estimate H-pol $\mathrm{T_B}$s at L-band using different profiles, where s, cl, P, SM and MSD represent root mean square height, correlation length, porosity, soil moisture, and moisture sensing depth, respectively.

linear moisture profile with a uniform weighting function. However, $\mathrm{T_B}$ was overestimated during the wet period, with higher RMSD of 10.37 K, as shown in Table V. Because the surface soil moisture is constrained by the C-band observations, the result

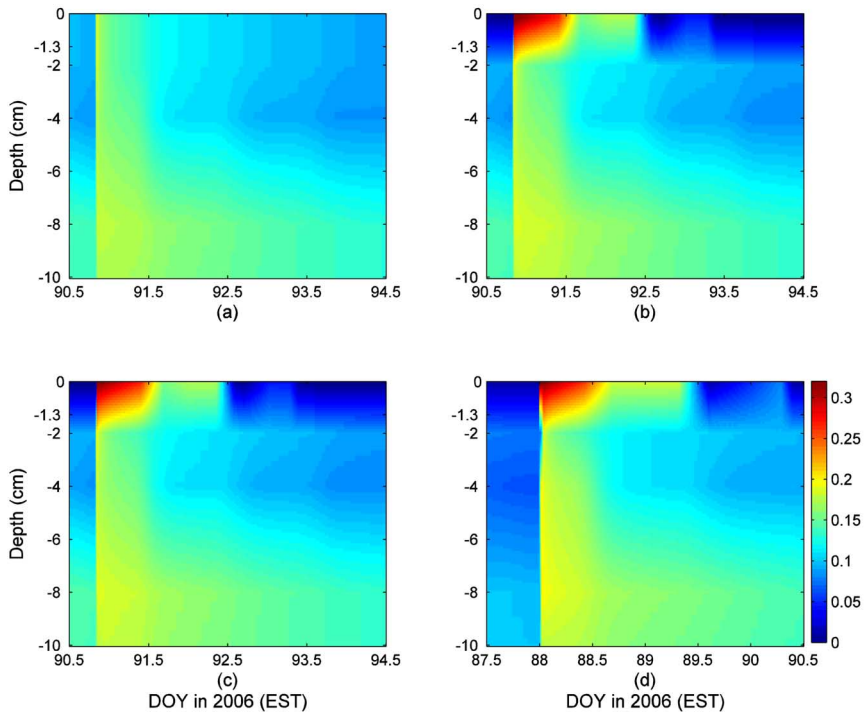

Fig. 10. The soil moisture profiles during the first drydown (DoY 90.5–94.5) (a) Constant in 0–2 cm using observed soil moisture (SM) at 2 cm, (b) SM in 0–2 cm obtained by linearly interpolating the SM in 0–2 mm estimated from C-band and observed SM at 2 cm, (c) SM in 0–2 cm obtained by linearly interpolating the SM in 0–1 mm estimated from C-band and observed SM at 2 cm; (d) SM profile during the second drydown (DoY 87.5–90.5), SM in 0–2 cm obtained by linearly interpolating the SM in 0–1 (wet period) or 0–2 mm (dry period) estimated from C-band and observed soil moisture at 2 cm. SM represents soil moisture and the colorbar shows the range of SM from 0.01–0.32 in $\mathrm{m}^3/\mathrm{m}^3$.

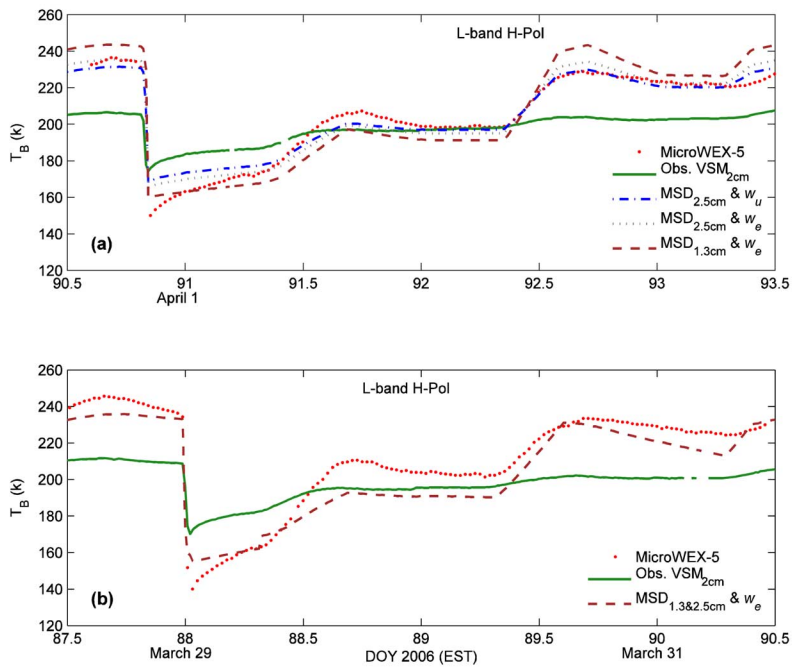

Fig. 11. Comparison $\mathrm{T_B}$ observed from MicroWEX-5 (dots) to those estimated using (a) observed soil moisture at 2 cm for e_p (solid line); moisture within MSD of 2.5 cm at L-band with uniform weighting function (w_u) for e_p (dash-dot line); moisture within MSD of 2.5 cm at L-band with exponentially decaying weighting function (w_e) for e_p (dotted line); and moisture within MSD of 1.3 cm at L-band with w_e for e_p (dashed line), during DoY 90.5–94.5. and (b) moisture within MSD of 1.3 and 2.5 cm at L-band during wet and dry periods, respectively, with w_e (dashed line), during DoY 87.5–90.5.

may indicate a need for using non-uniform weighting function such as an exponentially decaying function that would increase the contribution from the surface layer. It may also indicate that the MSD at C-band need to be shallower. In the next two profiles, we tested these hypotheses.

The *third moisture profile* was the same as second moisture profile, but with the soil moisture used for e_p obtained using an exponentially decaying weighting function. Overall, the $\mathrm{T_B}$ estimates, shown as the gray dashed line in Fig. 11(a), are very close to those obtained using the uniform weighting function,

TABLE V
ROOT MEAN SQUARE DIFFERENCES (RMSDS) AND STANDARD DEVIATIONS (SD) BETWEEN THE OBSERVED AND MODELED H-POL $\mathrm{T_B}$ AT L-BAND USING DIFFERENT MOISTURE PROFILES AND SOIL PROPERTIES OF ROOT MEAN SQUARE HEIGHT (s), CORRELATION LENGTH (cl) AND POROSITY DURING TWO DRYDOWN PERIODS

For drydown during DoY 90.5-94.5; wet period DoY 90.8-91.3; and dry period DoY 92.5-94.5									
Moisture profiles to estimate $\mathrm{T_B}$ @ L-band	s (cm)	cl (cm)	Porosity	RMSD in K			SD in K		
				Overall	Wet	Dry	Overall	Wet	Dry
Current approach (as in Fig.1)	0.62	8.72	0.37	19.19	20.99	22.42	15.67	3.55	3.63
Profile 1	0.41	8.72	0.55	19.18	19.56	23.65	15.67	3.51	3.62
Profile 2	0.41	8.72	0.55	4.53	10.37	2.64	4.52	3.96	2.46
Profile 3	0.41	8.72	0.55	4.55	7.31	3.65	4.50	4.02	2.67
Profile 4	0.41	8.72	0.55	9.14	4.11	10.27	8.60	4.14	3.59
For drydown during DoY 87.5-90.5; wet period DoY 88.0-88.3; and dry period DoY 89.5-90.5									
Profile 3 & 4	0.41	8.72	0.55	9.36	6.40	5.80	6.63	4.44	4.22

with a difference of RMSD within 1 K. However, during the wet period, immediately following the irrigation event, the exponentially decaying weighting improves the RMSD of $\mathrm{T_B}$ at L-band by 3 K, as shown in the Table V. During the dry period, the $\mathrm{T_B}$ using the exponential function has a higher RMSD than the $\mathrm{T_B}$s obtained using the uniform weighting by 1 K, because the drier surface layer contributes more than the deeper wet layers.

Even though using the exponentially decaying function improved the $\mathrm{T_B}$ estimates during the wet period, the $\mathrm{T_B}$s at the time of the event and within 12 hours have RMSDs are still high at about 7.3 K. This indicates that the MSD at C- and L-band may be shallower than 0–2 mm and 0–2.5 cm, respectively. The *fourth moisture profile* used a shallower surface layer, 0–1 mm, with its moisture estimated from the C-band. The 0–1 mm soil moisture was linearly interpolated with the moisture observed at 2 cm during MicroWEX-5, as shown in Fig. 10(c). The average soil moisture value used for e_p obtained using the exponentially decaying weighting function in the top 1.3 cm, the MSD at L-band. The $\mathrm{T_B}$ estimates, shown as the brown dashed line in Fig. 11(a), are closer to those observed within 12 hours after irrigation than the third moisture profile, with RMSDs reduced to 4.11 K, as shown in Table V. Decreasing the MSD at C-band to 1 mm and averaging the soil moisture using exponentially decaying weighting function in the top 1.3 cm for estimating $\mathrm{T_B}$ at L-band produced the best $\mathrm{T_B}$ estimates during the wet period.

The realistic estimates of $\mathrm{T_B}$ at L-band above, depended upon four assumptions: 1) the MSD of C-band is 1 mm and 2 mm during the wet and dry periods, respectively, with the soil moisture as low as 0.01 $\mathrm{m^3/m^3}$ during the driest period; 2) the MSD at L-band is 12.6 times that at C-band, using Mironov *et al.* (2009); 3) the soil moisture profile within the MSD at L-band is linear; and 4) the rough surface emissivity (e_p) at L-band can be adequately obtained using either a uniform or an exponentially decaying weighting function for an effective soil moisture value within the MSD. However, these assumptions may not be valid for different soil types or during different hydrological conditions. For example, the same approach was applied to the second drydown period, form DoY 80.5–90.5, in which the soil moisture within MSD at C-band of 0–1 mm for wet period, before DoY 88.3, and 0–2 mm for dry period was used along with the exponential weighting function to estimate e_p. The RMSDs of 2.34 and 2.60 K for H- and V-pol $\mathrm{T_B}$ at C-band, respectively, were obtained. The RMSDs were higher for the H-pol $\mathrm{T_B}$ at L-band compared to those obtained during the first drydown period, see Fig. 11(b) and V.

Because the moisture distribution within the MSD is highly dynamic during the wet period, particularly during the 12 hours following an irrigation event, a dynamic hydrological model such as LSM, NOAH, and LSP, is needed to provide detailed moisture profile in the soil column, with a vertical resolution sufficient for $\mathrm{T_B}$ estimation at L-band. Escorihuela *et al.* (2010) [35] used a hydrology model to obtain dynamic 0–2 cm soil moisture and found that the $\mathrm{T_B}$ estimates at L-band matched the observations. However, as discussed earlier, the vertical resolution of 0–2 cm was found to be too coarse for the sandy soils in this study. In addition, both the MSD and the weighting functions depend upon the soil moisture, and the use of one soil moisture value, assuming homogeneous soil surface, to estimate emissivity is unrealistic, particularly during hydrological extremes. Current microwave algorithms work fairly well during less dynamic stages of the drydown periods under hydrologic equilibrium. However, they provide unrealistic $\mathrm{T_B}$ estimates during hydrologic extremes. It is more important to know the hydrologic storage and fluxes during these periods because the response of the system is more significant than during the equilibrium periods. An improvement of about 20–30 K in $\mathrm{T_B}$ is needed, resulting in an improvement of 0.05–0.10 $\mathrm{m^3/m^3}$ in volumetric soil moisture during and immediately following a hydrological event to provide accurate estimates of the storage and fluxes using assimilation and retrieval algorithms from current space borne observations. In this study, the methods developed for bare soil using C- and L-band observations provide insights into the error sources in the current microwave algorithms during the highly dynamic periods. The observations from sensors such as AMSR-E and ASCAT are sensitive to moisture, porosity, and roughness at the surface, while those from SMOS and SMAP are sensitive to the soil properties in the lower layers. This study provides two recommendations to improve current microwave algorithms. First, using a dynamic hydrological model to provide detailed moisture profile within the MSD for the C- and L-band sensors, and second, developing a better approach to estimate e_p that utilizes the detailed moisture profile from the hydrological model. However, the operational use of the methodology needs further understanding of its computational demands and upscaling to the satellite scales.

V. Summary and Conclusions

This study aims to understand the impact of moisture dynamics within the sensing depth on L- and C-band brightness signatures in sandy soils. Current microwave algorithms use a single moisture value to represent the effective moisture in the moisture sensing depth that results in unrealistic $\mathrm{T_B}$ estimates for the bare and vegetated soil at L-band, particularly during extreme hydrologic conditions. C-band radiometric observations were used to estimate physically consistent surface parameters of sandy soils such as s, porosity, and moisture within the MSD at C-band, with the soil moisture of 0.01 $\mathrm{m^3/m^3}$ during the driest period. A uniform and an exponentially decaying weighting functions were used to obtain effective soil moisture values within the MSD at L-band for the rough surface emissivity (e_p) estimates of H-pol $\mathrm{T_B}$ at L-band. The results indicate that the impact of moisture distribution within the MSD on the $\mathrm{T_B}$ at L-band in sandy soils is more significant than that of physical properties, such as s, cl, and porosity. Reasonable estimates of $\mathrm{T_B}$ could be obtained when soil reached equilibrium, however large differences were obtained during the times of the events and early drydown stages.

It is almost impossible to accurately acquire soil moisture distribution within 0–2 cm using current state-of-the-art *in situ* sensors. A dynamic hydrological model such as LSM, NOAH, and LSP, may be used to provide detailed moisture profile in the soil column, with a vertical resolution sufficient for $\mathrm{T_B}$ estimation at L-band. Although such a method will increase the computational demands, current capabilities in high performance computing may allow such inclusions. In addition, the MSD and the weighting functions depend upon soil moisture. An improved approach that can use the detailed profile rather than one effective soil moisture value to estimate e_p is required.

Acknowledgment

The authors thank the anonymous reviewers for providing insightful comments and suggestions to improve the manuscript.

References

[1] J. Judge, "Microwave remote sensing of soil water: Recent advances and issues," *Trans. ASABE*, vol. 50, no. 5, pp. 1645–1649, 2007.

[2] E. Njoku, T. Jackson, V. Lakshmi, T. Chan, and S. Nghiem, "Soil moisture retrieval from AMSR-E," *IEEE Trans. Geosci. Remote Sens.*, vol. 41, no. 2, pp. 215–229, Feb. 2003.

[3] Z. Bartalis, V. Naeimi, S. Hasenauer, K. Scipal, H. Bonekamo, J. Figa, and C. Anderson, "Initial soil moisture retrievals from the METOP-A Advanced Scatterometer (ASCAT)," *Geophys. Res. Lett.*, vol. 34, no. L20401, 2007, doi 10.1029/2007GL031088.

[4] Y. Kerr, P. Waldteufel, J. Wigneron, S. Delwart, F. Cabot, J. Boutin, M. Escorihuela, J. Font, N. Reul, C. Gruhier, S. Juglea, M. Drinkwater, A. Hahne, M. Martín-Neira, and S. Mecklenburg, "The SMOS mission: New tool for monitoring key elements of the global water cycle," *Proc. IEEE*, vol. 98, no. 5, pp. 666–687, 2010.

[5] D. Entekhabi, E. Njoku, P. O'Neill, K. Kellogg, W. Crow, W. Edelstein, J. Entin, S. Goodman, T. Jackson, J. Johnson, J. Kimball, J. Piepmeier, R. Koster, N. Martin, K. McDonald, M. Moghaddam, S. Moran, R. Reichle, J. Shi, M. Spencer, S. Thurman, L. Tsang, and J. V. Zyl, "The soil moisture active passive (SMAP) mission," *Proc. IEEE*, vol. 98, pp. 704–716, 2010.

[6] Y. Du, F. Ulaby, and M. Dobson, "Sensitivity to soil moisture by active and passive microwave sensors," *IEEE Trans. Geosci. Remote Sens.*, vol. 38, no. 1, pp. 105–114, Jan. 2000.

[7] R. Lucas, J. Armston, R. Fairfax, R. Fensham, A. Accad, J. Carreiras, J. Kelley, P. Bunting, D. Clewley, S. Bray, D. Metcalfe, J. Dwyer, M. Bowen, T. Eyre, M. Laidlaw, and M. Shimada, "An evaluation of the ALOS PALSAR L-band backscatter-above ground biomass relationship Queensland, Australia: Impacts of surface moisture condition and vegetation structure," *IEEE J. Sel. Topics Appl. Earth Observ. Remote Sens. (JSTARS)*, vol. 3, no. 4-2, pp. 576–593, 2010.

[8] A. Balenzano, F. Mattia, G. Satalino, and M. Davidson, "Dense temporal series of C- and L-band SAR data for soil moisture retrieval over agricultural crops," *IEEE J. Sel. Topics Appl. Earth Observ. Remote Sens. (JSTARS)*, vol. 4, no. 2, pp. 439–450, 2011.

[9] R. Prakash, D. Singh, and N. Pathak, "A fusion approach to retrieve soil moisture with SAR and optical data," *IEEE J. Sel. Topics Appl. Earth Observ. Remote Sens. (JSTARS)*, vol. 5, no. 1, pp. 196–206, 2012.

[10] T. Schmugge and B. Choudhury, "A comparison of radiative transfer models for predicting the microwave emission from soil," *Radio Sci.*, vol. 16, no. 5, pp. 927–938, 1981.

[11] F. Ulaby, R. Moore, and A. Fung, *Microwave Remote Sensing: Active and Passive*. Boston, MA: Artech House, 1981, vol. I.

[12] M. Ek, K. Mitchell, Y. Lin, E. Rogers, P. Grunmann, V. Koren, G. Gayno, and J. D. Tarpley, "Implementation of NOAH land surface model advances in the National Centers for Environmental Prediction operational mesoscale Eta model," *J. Geophys. Res.*, vol. 108, no. D22, 2003, doi 10.1029/2002JD003296.

[13] R. Reichle, W. Crow, and C. Kepenne, "An adaptive ensemble Kalman filter for soil moisture data assimilation," *J. Geophys. Res.*, vol. 12, no. D09108, 2007, doi 10.1029/2006JD008033.

[14] J. Casanova and J. Judge, "Estimation of energy and moisture fluxes for dynamic vegetation using coupled SVAT and crop-growth models," *Water Res. Research*, vol. 44, no. W07415, 2008, doi 10.1029/2007WR006503.

[15] K. Schneeberger, M. Schwank, C. Stamm, P. de Rosnay, C. Mätzler, and H. Flühler, "Topsoil structure influencing soil water retrieval by microwave radiometry," *Vadose Zone J.*, vol. 3, pp. 1169–1179, 2004.

[16] M. Schwank, I. Völksch, J.-P. Wigneron, Y. Kerr, A. Mialon, P. de Rosnay, and C. Mätzler, "Comparison of two bare-soil reflectivity models and validation with L-band radiometer measurements," *IEEE Trans. Geosci. Remote Sens.*, vol. 48, no. 1, pp. 325–337, 2010.

[17] V. Mironov, L. Kosolapova, and S. Fomin, "Physically and mineralogically based spectroscopic dielectric model for moist soils," *IEEE Trans. Geosci. Remote Sens.*, vol. 47, no. 7, pp. 2059–2070, Jul. 2009.

[18] J.-P. Wigneron, Y. Kerr, P. Waldteufel, K. Saleh, M.-J. Escorihuela, P. Richaume, P. Ferrazzoli, P. de Rosnay, R. Gurney, J.-C. Calvet, J. Grant, M. Guglielmetti, B. Hornbuckle, C. Matzler, T. Pellarin, and M. Schwank, "L-band microwave emission of the biosphere (L-MEB) model: Description and calibration against experimental data sets over crop fields," *Remote Sens. Env.*, vol. 107, no. 4, pp. 639–655, 2007.

[19] J.-P. Wigneron, A. Chanzy, Y. Kerr, H. Lawrence, J. Shi, M. Escorihuela, V. Mironov, A. Mialon, F. Demontoux, P. de Rosnay, and K. Saleh-Contell, "Evaluating an improved parameterization of the soil emission in L-MEB," *IEEE Trans. Geosci. Remote Sens.*, vol. 49, no. 4, pp. 1177–1189, 2011.

[20] U. Wegmüller and C. Mätzler, "Rough bare soil reflectivity model," *IEEE Trans. Geosci. Remote Sens.*, vol. 37, no. 3, pp. 1391–1395, May 1999.

[21] A. Fung, *Microwave Scattering and Emission Models and Their Applications*. Norwood, MA: Artech House, 1994.

[22] J. Casanova, F. Yan, M. Jang, J. Fernandez, J. Judge, C. Slatton, K. Calvin, T. Lin, O. Lanni, and L. W. Miller, Field Observations During the Fifth Microwave, Water, and Energy Balance Experiment (MicroWEX-5): From March 9 Through May 26, 2006. Circular no. 1514, Tech. Rep., Ctr. Remote Sens., Univ. Florida, 2006 [Online]. Available: http://edis.ifas.ufl.edu/AE407

[23] J. Judge, J. Casanova, T.-Y. Lin, K.-J. C. Tien, M. Young Jang, O. Lanni, and L. Miller, Field Observations During the Second Microwave, Water, and Energy Balance Experiment (MicroWEX-2): From March 17 Through June 3, 2004. Circular no. 1480, Tech. Rep., Ctr. Remote Sens., Univ. Florida, 2004 [Online]. Available: http://edis.ifas.ufl.edu/AE360

[24] T. Yun Lin, J. Judge, K.-J. C. Tien, J. Casanova, M. Young Jang, O. Lanni, L. Miller, and F. Yan, Field Observations During the Third Microwave, Water, and Energy Balance Experiment (MicroWEX-3): From June 16 Through December 21, 2004. Circular no. 1481, Tech. Rep., Ctr. Remote Sens., Univ. Florida, 2004 [Online]. Available: http://edis.ifas.ufl.edu/AE361

[25] T. Bongiovanni, H. Enos, A. Monsivais-Huertero, B. Colvin, K. Nagarajan, J. Judge, P.-W. Liu, J. Fernandez-Diaz, R. D. R. Y. Goykhman, X. Duan, D. Preston, R. Shrestha, C. Slatton, M. Moghaddam, and A. England, Field Observations During the Eighth Microwave, Water, and Energy Balance Experiment (MicroWEX-8): From June 16 Through August 24, 2009, Tech. Rep., Ctr. Remote Sens., Univ. Florida, 2009 [Online]. Available: http://edis.ifas.ufl.edu/AE476

[26] J. Fernandes-Diaz, "Characterization of surface roughness of bare agricultural soils using Lidar," Ph.D. dissertation, Univ. Florida, Gainesville, FL, Dec. 2010.

[27] W. Burke, T. Schmugge, and J. Paris, "Comparison of 2.8- and 21-cm microwave radiometer observations over soils with emission model calculations," *J. Geophys. Res.*, vol. 84, no. C1, pp. 287–294, 1979.

[28] T. Mo and T. Schmugge, "A parameterization of the effect of surface roughness on microwave emission," *IEEE Trans. Geosci. Remote Sens.*, vol. GRS-25, no. 4, pp. 47–54, 1987.

[29] C. Prigent, J.-P. Wigneron, W. Rossow, and J. Pardo-Carrion, "Frequency and angular variations of land surface microwave emissivities: Can we estimate SSM/T and AMSU emissivities from SSM/I emissivities," *IEEE Trans. Geosci. Remote Sens.*, vol. 38, no. 5, pp. 2373–2386, 2000.

[30] J.-P. Wigneron, L. Laguerre, and Y. Kerr, "Simple modeling of the L-band microwave emission from rough agricultural soils," *IEEE Trans. Geosci. Remote Sens.*, vol. 39, no. 8, pp. 1697–1707, 2001.

[31] T. Pellarin, Y. Kerr, and J.-P. Wigneron, "Global simulation of brightness temperature at 6.6 and 10.7 GHz over land based on SMMR data set analysis," *IEEE Trans. Geosci. Remote Sens.*, vol. 44, no. 9, pp. 2492–2505, 2006.

[32] R. Panciera, J. Walker, and O. Merlin, "Improved understanding of soil surface roughness parameterization for L-band passive microwave soil moisture retrieval," *IEEE Geosci. Remote Sens. Lett.*, vol. 6, no. 4, pp. 625–329, 2009.

[33] K. Chen, T. Wu, L. Tsang, Q. Li, J. Shi, and A. Fung, "Emission of rough surfaces calculated by the integral equation method with comparison to three-dimensional moment method simulations," *IEEE Trans. Geosci. Remote Sens.*, vol. 41, no. 1, pp. 90–101, 2003.

[34] M. Dobson, F. Ulaby, M. Hallikainen, and M. El-Rayes, "Microwave dielectric behavior of wet soil—Part II: Dielectric mixing models," *IEEE Trans. Geosci. Remote Sens.*, vol. GE-23, no. 1, pp. 35–46, Jan. 1985.

[35] M. Escorihuela, A. Chanzy, J.-P. Wigneron, and Y. Kerr, "Effective soil moisture sampling depth of L-band radiometry: A case study," *Remote Sens. Env.*, vol. 114, pp. 995–1001, 2010.

Pang-Wei Liu received his B.S. and M.S. from Department of Geomatics, National Cheng-Kung University, Taiwan, in 2001 and 2003, and a M.S. from Department of Civil and Coastal Engineering, University of Florida in 2009. His master's research involved feature extraction from SAR images for change detection and evaluation of microwave signal attenuation in forest areas using LiDAR data sets. Pang-Wei is currently a PhD student in the Center for Remote Sensing, University of Florida. His research is focused on developing novel approaches to model active and passive microwave signatures for soil moisture retrieval and assimilation under bare soil and dynamic vegetation.

Roger D. De Roo (S'88–M'96) received the B.S. in Letters and Engineering degree from Calvin College, Grand Rapids, MI, in 1986, the B.S.E., M.S.E., and Ph.D. degrees from the University of Michigan in 1986, 1989, and 1996 respectively, all in electrical engineering. His dissertationtopic was on the modeling and measurement of bistatic scattering of electromagnetic waves from rough dielectric surfaces.

From 1996 to 2000, he was employed as a Research Fellow at the Radiation Laboratory in the department of Electrical Engineering and Computer Science (EECS) of the University of Michigan, investigating the modeling and simulation of millimeterwave backscattering phenomenology of terrain at near grazing incidence. He is currently an Assistant Research Scientist and Lecturer in the Department of Atmospheric, Oceanic, and Space Sciences (AOSS) at the University of Michigan. His current research interests include digital correlating radiometer technology development, radio frequency interference mitigation, inversion of geophysical parameters such as soil moisture, snow wetness and vegetation parameters from radar and radiometric signatures of terrain, and ground truth techniques for those geophysical parameters. He has supervised the fabrication of numerous dual-polarization microcontroller-based microwave radiometers.

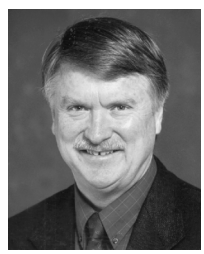

Anthony W. England (F'95) is Professor of Electrical Engineering and Computer Science, and of Atmospheric, Oceanic, and Space Sciences, College of Engineering, University of Michigan, Ann Arbor, and Interim Dean, College of Engineering and Computer Science, University of Michigan, Dearborn. He joined the University of Michigan in 1988. Tony earned his Ph.D. in geophysics from M.I.T. in 1970, and his research has spanned various aspects of microwave sensing of the Earth and planets, with recent emphasis upon microwave radiometry. He participated in and led geophysical field parties in Antarctica, used radar to study glaciers in Washington and Alaska, and used microwave radiometry to develop land-surface models of permafrost on the North Slope of Alaska. He was co-Investigator on the Apollo 17 Surface Electrical Properties experiment, co-Investigator on Shuttle Imaging Radar -A and -C, Mission Scientist for Apollo's 13 and 16, Mission Specialist astronaut on Spacelab 2, Space Station Program Scientist in 1986–87, and Visiting Professor at Rice University in 1987–88. He has been an Associate Editor for Journal of Geophysical Research, a member of the Administrative Committee of IEEE's Geoscience and Remote Sensing Society, a member of the National Research Council's Space Studies Board, and chair of several federal committees concerned with science and technology. He is Fellow of IEEE and member of AGU.

Jasmeet Judge (S'94–M'00–SM'05) received the PhD. degree in Electrical Engineering and Atmospheric, Oceanic, and Space Sciences from the University of Michigan, Ann Arbor, in 1999. She is currently the Director of the Center for Remote Sensing and an Associate Professor in the Agricultural and Biological Engineering Department in the Institute of Food and Agricultural Sciences, University of Florida, Gainesville. Her research interests are in microwave remote sensing applications to terrestrial hydrology for dynamic vegetation; modeling of energy and moisture interactions at the land surface and in the vadose zone; spatial and temporal scaling of remotely sensed observations in heterogeneous landscapes; and data assimilation. She is the Vice-chair of the National Academies' Standing Committee on Radio Frequencies and is a member of the Frequency Allocations in Remote Sensing Technical Committee in the IEEE-GRSS. She also serves the American Geophysical Union as the Chair of the Remote Sensing Technical Committee in the Hydrology Section.